Neuronal retrograde transport of Borna disease virus occurs in signaling endosomes

Caroline M. Charlier[1], Solène Debaisieux[2,&], Charlotte Foret[1], Anne Thouard[1], Giampietro Schiavo[2], Daniel Gonzalez-Dunia[1, #,*] and Cécile E. Malnou[1 #,*]

[1] Centre de Physiopathologie de Toulouse Purpan, INSERM UMR 1043, CNRS UMR 5282, Université Toulouse III Paul Sabatier, Toulouse, France;

[2] Molecular Neuropathobiology Laboratory, Sobell Department of Motor Neuroscience and Movement Disorders, UCL Institute of Neurology, University College London, London WC1N 3BG, United Kingdom.

[&] Present address: Department of Infection, UCL Cruciform Building, University College London, London WC1E 6BT, United Kingdom

[#]Contributed equally and should be considered joint last and corresponding authors

*To whom correspondence should be addressed. Email: daniel.dunia@inserm.fr, cecile.malnou@inserm.fr, Phone: +33 5 62 74 45 11

Running title: Bornavirus axonal transport

Keywords: Bornavirus, neuron, axonal transport, signaling endosomes

Word count:

Summary: 174

Main text:

Abbreviations: BDNF: Brain-Derived Neurotrophic Factor; BDV: Borna Disease Virus; CNS: Central Nervous System; ER: Endoplasmic Reticulum RNP: RiboNucleoParticle; TeNT: Tetanus neurotoxin.

Summary

Long-range axonal retrograde transport is a key mechanism for the cellular dissemination of neuro-invasive viruses, such as Borna Disease Virus (BDV), for which entry and egress sites are usually distant from the nucleus, where viral replication takes place. Although BDV is known to disseminate very efficiently in neurons, both *in vivo* and in primary cultures, the modalities of its axonal transport are still poorly characterized. In this work, we combined different methodological approaches, such as confocal microscopy and biochemical purification of endosomes, to study BDV retrograde transport. We demonstrate that BDV ribonucleoparticles (composed of the viral genomic RNA, nucleoprotein and phosphoprotein), as well as the matrix protein, are transported towards the nucleus into endocytic carriers. These specialized organelles, called signaling endosomes, are notably used for the retrograde transport of neurotrophins and activated growth factor receptors. Signaling endosomes have a neutral luminal pH and thereby offer protection against degradation during long-range transport. This particularity could allow the viral particles to be delivered intact to the cell body of neurons, avoiding their premature release in the cytoplasm.

Introduction

Borna Disease Virus (BDV) is a non-segmented, negative-stranded RNA virus belonging to the *Bornaviridae* family. Its 8.9 kb genome, the smallest of the *Mononegavirales* order, encodes only six proteins (de la Torre, 1994): the nucleoprotein (N), the viral polymerase (L) and its cofactor the phosphoprotein (P), the matrix protein (M), the glycoprotein (G) and the non-structural small protein X. The enveloped virion contains the ribonucleoparticle (RNP), composed of the viral genomic RNA encapsidated into BDV N, in interaction with BDV L, P and M proteins. The envelope is composed of a membrane in which are found the two isoforms of BDV G (84 and 43 kDa) (Gonzalez-Dunia *et al.*, 1998).

In vivo, BDV preferentially targets neurons of the central nervous system (CNS), although it can infect a large variety of cell types *in vitro* (de la Torre, 2002, Gonzalez-Dunia *et al.*, 2005). It has the particularity, unique among *Mononegavirales*, to replicate in the nucleus of infected cells without developing any cytopathic effect. Despite numerous studies, some steps of its replication cycle remain, however, unknown. In particular, receptor-mediated entry, retrograde transport to the nucleus, virion assembly and release are not well characterized (Lipkin *et al.*, 2011). Following interaction with a still unknown receptor, BDV enters the cell via clathrin-dependent endocytosis to form a vesicle that fuses with an early endosome. Then, acidification of the late endosome allows the fusion between viral and endosomal membranes and RNP release (Clemente *et al.*, 2009). After genome replication and protein synthesis, the precise modalities of virion assembly are still unknown. In particular, whether RNPs follow an anterograde transport route in an enveloped form or naked is not known, and even if neuron-to-neuron transmission occurs with enveloped virions and/or with non-enveloped RNPs (Clemente *et al.*, 2007). Previous work from our team allowed the observation of BDV RNP trafficking in non-neuronal cells by the use of a recombinant fluorescent-tagged virus (Charlier *et al.*, 2013). In neurons, however, one important feature of the BDV replication cycle is the necessity of a long-range retrograde and anterograde transport via the axonal route, since entry and egress sites are often distant from the cell body, where viral replication takes place.

Axonal transport is a key mechanism for neuroinvasive pathogens (Taylor *et al.*, 2015). Indeed, the long distances separating somas from nerve terminals imply that neurotropic viruses must use specialized molecular motors to move in a vectorial manner along axons and cannot solely rely on passive diffusion. Two principal strategies for axonal retrograde

transport are described for pathogens (Salinas *et al.*, 2010). The first one is to directly recruit molecular motors, such as cytoplasmic dynein or its associated complex dynactin, as exemplified by Herpes Simplex Virus type 1 (HSV-1). After membrane fusion, HSV-1 naked particle is released into the cytoplasm. Several proteins of the tegument then recruit dynein, dynactin, and adaptor proteins, allowing a rapid retrograde transport along microtubules (Diefenbach *et al.*, 2008). Another strategy for axonal trafficking is to use vesicular transport. Indeed, membrane organelles, such as endocytic and exocytic vesicles, constantly travel along axons and several pathogens access these organelles to spread in the CNS. This is for example the case for Canine Adenovirus type 2 (CAV-2), which enters the cell by receptor-mediated endocytosis before traveling into axonal endosomes (Salinas *et al.*, 2009). Another well documented example is tetanus neurotoxin (TeNT), which also uses the vesicular pathway to be transported in neurons (Lalli *et al.*, 2003). These endocytic structures, also called signaling endosomes, are usually responsible for the transport of neurotrophins, such as nerve growth factor or brain-derived neurotrophic factor (BDNF), as well as of their corresponding receptors $p75^{NTR}$ and TrkB (Bucci *et al.*, 2014). An important characteristic of these vesicles is that their luminal pH is close to neutral (Bohnert *et al.*, 2005). This allows cargoes to be transported over long distances in a protective environment, avoiding pH-dependent conformational changes. Neutral axonal endosomes could therefore constitute an ideal transport pathway for neurotropic viruses to reach the cell body without destabilization of the viral particle, preventing membrane fusion and premature release of the viral genome (Salinas *et al.*, 2010).

Although BDV is known to disseminate particularly well in neurons, both *in vivo* in the CNS and *in vitro* in neuronal primary cultures or in organotypic hippocampal slices (Bajramovic *et al.*, 2003, Daito *et al.*, 2011a, Wu *et al.*, 2013), the modalities of its axonal transport are still poorly characterized. So far, no study has described any direct interaction between a component of the BDV particle and a molecular motor. Moreover, BDV entry follows a receptor-dependent endocytosis pathway that requires the small GTPase Rab5 (Clemente *et al.*, 2009), a protein also implicated in the transport of axonal endosomes (Deinhardt *et al.*, 2006). These data argue for the hypothesis that BDV particles could be transported into signaling endosomes. In this work, we combined different methodological approaches, based on colocalization studies and biochemical purification of endosomes, to determine whether BDV uses such vesicular pathway for its retrograde axonal transport.

Results

BDV particles and TeNT colocalize in axonal vesicles. In a first attempt to investigate whether BDV particles are transported along axonal endosomes, we sought to perform colocalization studies between BDV and known axonal cargoes. Among well-described axonal cargoes, TeNT undergoes specific uptake and retrograde transport in axonal endosomes (Lalli *et al.*, 2002). Here, we used the binding fragment of tetanus neurotoxin (H_CT), coupled to Alexa Fluor 555 (H_CT-555), which is as a very reliable tool to monitor axonal retrograde transport of signaling endosomes (Lalli *et al.*, 1999, Lalli *et al.*, 2002, Debaisieux *et al.*, 2016). Therefore, we performed colocalization studies between H_CT-555 and BDV particles in fixed neurons.

To this aim, we used primary cultures of hippocampal neurons, which present long axons allowing easy detection of BDV particles. By performing preliminary kinetic analyses of infection, we determined that a punctate staining, likely corresponding to BDV particles, was best detected in axons eight to ten days after virus inoculation (data not shown). We thus labeled neurons with H_CT-555 at ten days post-infection before proceeding to colocalization studies. We performed indirect immunofluorescence experiments against BDV N or P proteins, the two main components of BDV RNPs, and colocalization analyses with H_CT-555 were performed by confocal microscopy (Fig. 1A and 1B, upper panels). In parallel, neurons were stained for β–III tubulin, to verify the axonal integrity (data not shown). Each colocalization event was confirmed by drawing an intensity profile (Fig. 1A and 1B, lower panels). To determine the colocalization percentages between BDV N or P and H_CT-555, we analyzed all the vesicles containing BDV N or P proteins. Among them, we determined the proportion which was also positive for H_CT-555 (Fig. 1C). We observed that around 75% of BDV N-containing vesicles and 65% of BDV P-containing vesicles were also positive for H_CT-555. These first results argue for a transport of BDV in axonal endosomes in cultured hippocampal neurons.

Biochemical approaches to purify axonal endosomes. We next decided to complete these results by a biochemical approach based on the purification of axonal endosomes and the analysis of their protein content (Fig. 2). Primary cultures of cortical neurons were infected by BDV, or left non-infected as a control, and maintained for 13 days, a time necessary to allow BDV spreading to the entire culture, as demonstrated in previous studies (Bajramovic *et al.*,

2003). They were then submitted to either whole cell lysis, or gentle cell lysis to preserve cellular organelles, notably axonal endosomes (see Fig. 2 and Experimental Procedures). We next used two complementary methods to obtain axonal endosome-enriched fractions (Fig. 2). The first one consisted in performing immunoprecipitation against Trk receptors, which are markers for axonal endosomes (Method 1) (Bucci *et al.*, 2014). The second one consisted of flow cytometry-based sorting of axonal endosomes labelled by fluorescent H_CT that was beforehand pre-incubated with neurons (Method 2).

Axonal endosomes obtained by immunoprecipitation contain BDV proteins. We first sought to purify axonal endosomes by performing immunoprecipitation experiments using a pan-Trk antibody. This antibody recognizes the cytoplasmic portion of Trk receptors, the cellular receptors of several neurotrophins, including BDNF, which localize in axonal endosomes (Lalli *et al.*, 2002). The protein content of the immunoprecipitates was then analyzed by western blotting (Fig. 3).

We first carried out control experiments in which we performed a whole cell lysis of non-infected or infected neurons, leading to the disruption of all cellular organelles, including axonal endosomes (Fig. 3). As expected, we observed the presence of TrkB in the immunoprecipitates (Figure 3A). Another endosomal marker, Rab7 (Chavrier *et al.*, 1990), which does not interact with Trk receptors, was also detected in the input fractions, but not in the immunoprecipitates, confirming that axonal endosomes had indeed been disrupted during cell lysis. Moreover, BDV N, P, G and M proteins were not found in the immunoprecipitate obtained from infected neurons, indicating that they do not directly interact with Trk receptors (Fig. 3A).

We repeated the same anti pan-Trk immunoprecipitation experiment after having performed a gentle cell lysis to preserve axonal endosomes (Fig. 3B). In this case, Rab7 was found associated to the Trk immunoprecipitates, in contrast to what was observed with whole cell lysis, indicating that this method allows the preservation of axonal endosome integrity. Moreover, BDV N, P, G and M were also found in the immunoprecipitates obtained from infected neurons, indicating that BDV proteins are present in the axonal endosome-enriched fraction.

However, we reasoned that this purification method based on the isolation of Trk-containing endosomes might not be optimal. Indeed, Trk receptors follow the classical secretory pathway. As such they transit through the endoplasmic reticulum (ER) and Golgi apparatus after synthesis before reaching the plasma membrane. As a matter of fact, western

blot experiments revealed that markers such as GM-130 (Golgi Matrix protein of 130 kDa), ERGIC (ER Golgi Intermediate Compartment) and calnexin (ER) (Schweizer *et al.*, 1988, Wada *et al.*, 1991, Marra *et al.*, 2001) were also present in our immunoprecipitates (Fig. 3C), suggesting that the immunoprecipitates of Trk-containing axonal endosomes may also contain other subcellular organelles.

Flow cytometry-sorted axonal endosomes contain BDV proteins and the viral genome. We thus decided to develop an alternative approach to purify axonal endosomes with greater efficiency. To this aim, we developed a biochemical approach based on flow cytometry sorting of fluorescently-labeled endosomes. Similar to our colocalization studies (see Fig. 1), we used H_CT as an endosomal probe, which was labeled with Alexa Fluor 647 dye for its detection by flow cytometry (H_CT-647).

Considering the expected size of axonal endosomes (between 100 and 1 μm), we first calibrated our flow cytometer for the detection of small particles. Latex particles of distinct known sizes (0.1, 0.5, 1 and 3 μm) were used to set up the flow cytometer FSC and SCC parameters. We next observed that we could also detect and discriminate fluorescent standard microbeads of 0.5, 0.9 and 3 μm (data not shown). Next, we analyzed cell homogenates obtained by gentle cell lysis of non-infected neurons that had been previously incubated with H_CT-647. Flow cytometry analysis of the crude cell homogenates revealed a population of events with a relatively continuous size and granulometry distribution (Fig. 4A, left panel). These events were size-gated into three populations, designated as P1 to P3, that were then analyzed for fluorescence intensity and count number (Fig. 4A). Alexa 647-positive events were then gated and sorted to obtain F1 and F2 fractions. As expected, no fluorescent events were detected in a control experiment using neurons that had not been exposed to H_CT-647 (Fig. 4B).

We next analyzed the protein content of the sorted endosome-containing fractions obtained from non-infected or infected neurons. We focused on the F1 fraction, because it mostly contains fluorescent events (>86%). Moreover, the paucity of the material present in F2 fractions (680 fluorescent positive events sorted in F2 fraction *vs.* 2,880 in F1 fraction) limited the protein content available for western blotting experiments. In F1 fractions sorted from non-infected neurons, western blot analysis revealed the presence of the axonal endosome markers TrkB and Rab7, suggesting that this method allowed the purification of preserved axonal endosomes (Fig. 5A, left panel). When a similar analysis was performed using infected neurons, we also detected the presence of BDV N, P and M proteins in addition

to TrkB and Rab7 (Fig. 5A, right panels). We, however, did not succeed in detecting BDV G isoforms, probably due to the limiting amounts of protein content, together with the fact that anti-BDV G antibody is not as sensitive as the other anti-BDV antibodies used in this study (data not shown). Moreover, in contrast to the results obtained with the immuno-purification of Trk-containing endosomes, western blot analysis of F1-sorted fractions revealed that they were negative for GM-130, calnexin or ERGIC antigens (Fig. 5B), suggesting that such a flow cytometry-based sorting allows a more stringent purification of axonal endosomes.

Lastly, we investigated whether BDV genomic RNA was also found in F1-sorted fractions. We purified total RNAs from F1 fractions and performed a reverse-transcription experiment targeting the viral (negative sense) genomic RNA. The resulting cDNAs were then amplified by PCR, using BDV-specific primers. As shown in Fig. 5C, a DNA fragment at the expected size of 360 bp was amplified specifically in F1 fractions obtained from infected neurons, demonstrating that the viral genomic RNA is present in axonal endosomes, in addition to the above-mentioned BDV proteins.

Discussion

One requirement for neurotropic viruses to disseminate efficiently into the CNS is that viral proteins, genome and/or particle must move over long distances along axons, a highly specialized neuronal compartment. Although the strong neuroinvasive properties of BDV have been observed long ago, either in animal models or using *in vitro* systems (Bajramovic *et al.*, 2003, Daito *et al.*, 2011a, Wu *et al.*, 2013), the strategy adopted by this virus upon infection to reach the neuronal nucleus, where viral replication takes place, still remains a mystery. In this study, we sought to gain further insights into the modalities of BDV axonal transport.

Colocalization studies performed by confocal microscopy on hippocampal axons indicated that approximately 70% of BDV antigen-containing puncta were also positive for H_CT, a probe specific for axonal endosomes (Lalli *et al.*, 2003, Salinas *et al.*, 2010). This result is comparable to what has been observed with CAV-2, another virus described to travel in signaling endosomes in motor neurons (Salinas *et al.*, 2009), and therefore constitutes a strong argument in favor of BDV being recruited to axonal transport carriers. The remaining 30% of BDV antigen-containing puncta that are negative for H_CT could have stochastically internalized BDV and not H_CT. It is also possible that part of this staining corresponds to vesicles containing newly synthesized BDV virions (or RNPs) that are traveling in an

anterograde direction and thus do not contain H_CT. Indeed, even if a punctate axonal staining for BDV antigens is usually observed at early stages after infection, we cannot exclude the possibility that neo-synthetized virions may also be present in neurons, since our immunofluorescence analyses have been performed ten days post-infection, a time sufficient to allow production of new viral progeny. Indeed, given the paucity of cell-free virus produced by BDV-infected cells, it is unfortunately not possible to use a stronger multiplicity of infection and visualize viral spread at earlier time points.

We next decided to perform biochemical purification of Trk-containing endosomes, taking advantage of an experimental strategy used by several groups for the study of signaling endosomes (Mitchell *et al.*, 2012 , Zhou *et al.*, 2012). By this method, we were able to detect axonal endosome markers, such as TrkB and Rab7 in the immunoprecipitates, validating this experimental approach. Moreover, BDV N, P, M and G proteins were also found in the immunoprecipitates. However, a key feature of axonal transport is that cellular proteins that will ultimately be transported in a retrograde manner, such as Trk receptors themselves, must first be delivered to the axon terminus. Consequently, Trk receptors first follow the classical cellular secretory pathway, transiting via ER and Golgi apparatus and reach the axon terminus by anterograde transport (Ascano *et al.*, 2009). Thus, immunoprecipitation of Trk-containing endosomes not only purifies endosomes that move in the retrograde direction but also vesicles that are delivered to the axon plasma membrane, as well as ER- and Golgi-derived microsomes. Control western blot experiments indeed showed that ER and Golgi proteins were present in pan-Trk immunoprecipitates. In any event, as BDV N, P and M are directly translated into the cell cytoplasm and not on ER-associated ribosomes, our results clearly demonstrate that these proteins are found in axonal endosomes. For BDV G, however, results need to be interpreted with caution. Indeed, BDV G follows the cellular secretory pathway and both the entire protein and its two cleaved isoforms associate with ER and Golgi (Daito *et al.*, 2011b). We therefore cannot rule out the possibility that part of BDV G may actually be immunoprecipitated from ER- and Golgi-derived microsomes.

Flow cytometry-based sorting of H_CT-containing vesicles allowed to definitively conclude that BDV components were actually transported by axonal endosomes. Clearly, H_CT represents a more stringent marker of axonal endosomes than Trk receptors, since it only follows retrograde transport and does not transit through the ER or Golgi (Lalli *et al.*, 2003, Salinas *et al.*, 2010). As a matter of fact, no trace of ER or Golgi apparatus markers were found in the sorted fractions, confirming the reliability of H_CT as an axonal endosome probe. This also demonstrates that the use of a cell cracker is indeed appropriate to obtain intact

endosomes, since it has been suggested that the mechanical forces applied for cell fractionation might create hybrid membrane vesicles (Salomon *et al.*, 2010).

Since BDV N, P and M proteins, as well as the viral genome, were all detected in sorted H_CT positive fractions, it is very likely that BDV RNPs are actually present in axonal endosomes. We, however, were unable to detect BDV G by western blot. We thus cannot conclude whether BDV particles are transported along axonal endosomes in an enveloped or uncoated form. In neuronal primary cultures, BDV spreads without any detectable extracellular virus or syncytium formation (Bajramovic *et al.*, 2003) and the precise contribution of BDV G in neuronal spread remains debated (Clemente *et al.*, 2007). One current hypothesis proposes two modes of virus propagation into neurons: a primary infection that depends on the binding of BDV G to its receptor, followed by a cell-to-cell viral spread that would not necessarily require the BDV G protein (Lennartz *et al.*, 2016).

Another common pathway between H_CT and BDV is the initial association with $Rab5^-$ positive early endosomes. This is particularly interesting when considering that there are clear functional differences between axonal endosomes and endocytic organelles found in epithelial cells. Notably, in contrast to epithelial cells, Rab7-positive axonal endosomes display a neutral luminal pH (Bohnert *et al.*, 2005, Salinas *et al.*, 2009). By transiting through such non-acidic axonal endosomes, BDV particles could remain efficiently associated with long-range transport vesicles until being delivered to the soma, triggering the exit of the viral material from these compartments. As such, neutral axonal endosomes may offer an efficient protection against degradation during long-range transport, allowing the viral particle to be delivered intact to the cell body of neurons. This might also explain why BDV disseminates much better in primary neuronal cultures when compared to other cell types. In non-neuronal cell types, the cell-to-cell spread of BDV is relatively inefficient, as attested by the paucity of BDV fluorescent particles routing to the nucleus detected in our recent study, which had been performed in epithelial Vero cells (Charlier *et al.*, 2013). This may actually be explained by the fact that BDV particles would be prematurely released into the cytoplasm, due to the early acidification of endosomes.

Recently, a proteomic analysis of the composition of signaling endosomes revealed that they contain many proteins, notably receptors, which play key roles in infection and spread of many neurotropic viruses (Debaisieux *et al.*, 2016). Such knowledge may now provide new leads towards the identification of the cellular receptor for BDV, thereby contributing to a better understanding of BDV neuropathogenesis.

Experimental procedures

Ethics statement. Animal handling and care for the preparation of primary neuronal cultures were performed in agreement with the European Union Council Directive 86/609/EEC and experiments were done following the French national chart for ethics of animal experiments (articles R 214- 87 to 90 of the "Code rural"). Our protocol received approval from the local committee on the ethics of animal experiments (permit number: 04-U1043-DG-06). Rats were deeply anesthetized with CO_2 before euthanasia.

Primary neuronal cultures and virus infection. Before seeding, supports were coated with 500 µg/ml poly-ornithine (Sigma), followed by 5 µg/ml laminin (Roche). Primary cortical neurons were prepared from Sprague-Dawley rat embryos at gestational day 17 by the papain dissociation method as described previously (Bonnaud *et al.*, 2015). Hippocampal neurons were prepared from newborn Sprague-Dawley rats as described (Prat *et al.*, 2009). Neurons were maintained in Neurobasal medium (Invitrogen) supplemented with 100 µg/ml penicillin/streptomycin, 2 mM glutamine, 2 % B-27 supplement (Invitrogen) and 1 % fetal calf serum for hippocampal neurons. Neuronal cultures contained more than 90 % neurons, as assessed by staining with the neuron-specific marker ß-III tubulin (data not shown).

Neurons were infected one day after plating with cell-free BDV. Cell-released virus stocks were prepared as described using Vero cells persistently infected by wild-type BDV (Giessen strain He/80) (Prat *et al.*, 2009). Efficient BDV infection of neurons was verified by indirect immunofluorescence for each experiment.

Labeling of axonal endosomes with H_CT. To visualize axonal endosomes by confocal microscopy, hippocampal neurons were incubated with the binding fragment of TeNT (H_CT) that was coupled with Alexa Fluor 555 dye (H_CT-555), as described previously (Lalli *et al.*, 2002). Incubation was performed with 10 nM H_CT-555 during 1 h at 37 °C in Neurobasal medium. To eliminate the excess of non-internalized toxin that could remain bound to cell surface receptors, one acid wash was then performed during 1 min on ice with a solution containing 100 mM citric acid and 142 mM NaCl (pH = 2), followed by two washes in PBS (Invitrogen).

To perform flow cytometry analysis and sorting, cortical neurons were incubated with H_CT coupled with Alexa Fluor 647 dye (H_CT-647). Incubation was performed in Neurobasal medium containing 20 nM H_CT-647, during 3 h at 37°C, followed by a 10 min incubation on ice. One acid wash was then, followed by two washes with Hank's Buffered Salt Solution (HBSS, Invitrogen) supplemented with protease inhibitors.

Indirect immunofluorescence analysis. Neurons were fixed with 2 % paraformaldehyde at room temperature for 10 min then with 4 % paraformaldehyde for 10 min. They were then washed three times with PBS and permeabilized with PBS containing 0.1 % Triton-X100 during 4 min. After two washes with PBS, non-specific antigenic binding sites were blocked with 2.5 % normal goat serum (Invitrogen) during at least 1 h. Rabbit antisera recognizing BDV N or P proteins (Bonnaud *et al.*, 2015) were diluted in PBS containing 2.5 % normal goat serum and incubated 1 h at room temperature. After three washes with PBS (containing 0.1 % Triton-X100 in the first one), neurons were incubated with secondary goat anti rabbit antibody coupled to Alexa Fluor 488 during 1 h at room temperature. After three washes, coverslips were mounted onto microscope slides using Vectashield mounting medium (Vector laboratories) containing DAPI. Images were acquired on a LSM 710 confocal microscope (Zeiss) using fixed acquisition parameters and a 63x objective. Image J software was used for colocalization analyses.

Preparation of cell extracts. For whole cell extract preparation, neurons were washed twice with PBS, scrapped and centrifuged for 5 min at 170 x g at 4 °C. Cell pellets were suspended in lysis solution containing 500 mM Tris-HCl pH 8, 150 mM NaCl, 0.1 % SDS, 1 % Nonidet P-40, 0.5 % sodium deoxycholate, 1 mM sodium orthovanadate and protease inhibitors (Complete mini, Roche), an incubated for 30 min at 4 °C. Lysates were then centrifuged at 16000 *x g* for 20 min at 4 °C to eliminate cellular debris.

To preserve endosome integrity before immunoprecipitation, a gentle cell lysis was performed as follows. After two washes with HBSS containing protease inhibitors, neurons were scrapped and centrifuged for 5 min at 170 *x g* and 4 °C. Cell pellets were resuspended in Breaking Buffer (BB) containing 10 mM Hepes pH 7.2, 0.25 M sucrose, 1 mM EDTA, 1 mM magnesium acetate and protease inhibitors. Gentle lysis was achieved by 15 passages through a Cell cracker (18 µm clearance, EMBL Technology Transfer, GmbH). Homogenates were clarified by centrifugation at 690 *x g* during 15 min at 4 °C and kept at -80 °C for further analyses.

To perform flow cytometry-based sorting, the following lysis buffer was used: 25 mM MES (2-(N-morpholino)-ethanosulfonic acid), 150 mM NaCl, 5 mM EDTA and protease inhibitors at pH 6.5 (Chasan *et al.*, 2013).

Immunoprecipitation experiments. Protein concentrations of the extracts were determined using a Bradford assay. Then 250 µg were used for all experiments, diluted in a final volume of 500 µl of BB. Lysates were pre-cleared during 30 min at 4°C using 50 µl µMACS protein G microbeads (Miltenyi Biotec). In parallel, 2 µg of goat anti pan-Trk antibodies (Santa-Cruz Biotechnologies) were coupled with 50 µl µMACS protein G microbeads (Myltenyi Biotec), then washed with BB and passed on a magnetic column (µ Columns, Myltenyi Biotec). After removal from the magnetic field, the precleared lysates were mixed with the coupled microbeads and incubated for 2 h at 4°C. After four washes on the magnetic column, elution of immunoprecipitates was performed by boiling with 60 µl of Laemmli buffer.

Flow cytometry analysis and sorting. H_cT-647-labeled neuronal extracts obtained after gentle lysis were analyzed and sorted by flow cytometry using a FACSARIA II SORP (BD Biosciences) equipped with DIVA software, using a protocol adapted from (Chasan *et al.*, 2013). Calibration was performed with size standard latex microbeads of 0.1, 0.5, 1 and 3 µm and 0.5, 0.9 and 3 µm FITC microbeads (Biocytex) and the fluid sheath running through the cytometer was filtered before use. Samples were analyzed at a speed of 500 to 1,000 events/sec. A minimum of 10,000 events was collected for analysis. Data were analyzed using the FlowJo software (Tree Star).

Western blotting. Western blots were performed as previously described (Prat *et al.*, 2009), by using the following primary antibodies: rabbit sera anti BDV N, P, M and G (kindly provided by Martin Schwemmle for BDV M and Keizo Tomonaga for BDV G antibodies), rabbit anti Trk B antibody (Santa-Cruz Biotechnology), anti Rab7 antibody (Cell Signaling Technology), anti calnexin antibody (Enzo Life Sciences), anti GM-130 antibody (BD Biosciences) and mouse monoclonal anti ERGIC antibody (Sigma Aldrich). The secondary antibodies used were anti-rabbit and anti-mouse antibodies coupled to 680 nm and 770 nm infrared dyes (Biotium). Laser scanning of blots and analyses were performed using the Odyssey Infrared Imaging System (Li-Cor).

Detection of BDV genomic RNA by reverse-transcription and PCR. Total RNAs were extracted from input or sorted fractions using the RNeasy micro kit (Qiagen), following the manufacter's instructions. RNAs were reverse-transcribed using SuperScript III Reverse Transcriptase (Life Technologies) with a primer specific for genomic viral RNA (primer sequence: 5'GACACTACGACGGGAACGAT3'). The resulting cDNAs were then submitted to PCR analysis using BDV-specific primers (forward primer: 5'CGGTAGACCAGCTCCTGAAG3', reverse primer: 5'GAGGTCCACCTTCTCCATCA3'), using Phusion DNA polymerase (Fermentas) and the following cycles: 3 min at 98 °C, then 30 cycles with 10 sec at 98 °C, 10 sec at 55 °C, 15 sec at 72 °C, and a final incubation of 5 min at 72 °C.

Acknowledgments

We thank the staff of the different facilities of our research center (Sophie Allart and Astrid Canivet at the cellular imaging facility and Fatima L'Faqihi-Olive and Valérie Duplan-Eche at the flow cytometry platform) for excellent technical assistance that was instrumental for the proper realization of this project. We thank Arnaud Justin for technical assistance. We are grateful to Roland Liblau and Abdelhadi Saoudi for critical reading of the manuscript and insightful comments.

This work was supported by grants from ANR (ANR-10-Blanc-1322, to DGD), the Fondation pour la Recherche Médicale (Equipe FRM 2009, to DGD), and institutional grants from INSERM and CNRS (to DGD). This work is part of the Ph.D. thesis work of CMC, who was supported by a doctoral fellowship from the Ministère de l'Enseignement Supérieur et de la Recherche. The funders had no role in study design, data collection and analysis, decision to publish, or preparation of the manuscript.

Competing Interests

The authors have declared that no competing interests exist.

Author Contributions

Conceived and designed the experiments: CMC, SD, GS, DGD, CEM. Performed the experiments: CMC, SD, CF, AT, CEM. Analyzed the data: CMC, DGD, CEM. Wrote the paper: DGD, CEM.

References

Ascano, M., Richmond, A., Borden, P. and Kuruvilla, R. (2009). Axonal targeting of Trk receptors via transcytosis regulates sensitivity to neurotrophin responses. *J Neurosci* **29,** 11674-11685.

Bajramovic, J.J., Munter, S., Syan, S., Nehrbass, U., Brahic, M. and Gonzalez-Dunia, D. (2003). Borna disease virus glycoprotein is required for viral dissemination in neurons. *J Virol* **77,** 12222-12231.

Bohnert, S. and Schiavo, G. (2005). Tetanus toxin is transported in a novel neuronal compartment characterized by a specialized pH regulation. *J Biol Chem* **280,** 42336-42344.

Bonnaud, E.M., Szelechowski, M., Betourne, A., Foret, C., Thouard, A., Gonzalez-Dunia, D. and Malnou, C.E. (2015). Borna disease virus phosphoprotein modulates epigenetic signaling in neurons to control viral replication. *J Virol* **89,** 5996-6008.

Bucci, C., Alifano, P. and Cogli, L. (2014). The role of rab proteins in neuronal cells and in the trafficking of neurotrophin receptors. *Membranes (Basel)* **4,** 642-677.

Charlier, C.M., Wu, Y.J., Allart, S., Malnou, C.E., Schwemmle, M. and Gonzalez-Dunia, D. (2013). Analysis of borna disease virus trafficking in live infected cells by using a virus encoding a tetracysteine-tagged p protein. *J Virol* **87,** 12339-12348.

Chasan, A.I., Beyer, M., Kurts, C. and Burgdorf, S. (2013). Isolation of a specialized, antigen-loaded early endosomal subpopulation by flow cytometry. *Methods Mol Biol* **960,** 379-388.

Chavrier, P., Parton, R.G., Hauri, H.P., Simons, K. and Zerial, M. (1990). Localization of low molecular weight GTP binding proteins to exocytic and endocytic compartments. *Cell* **62,** 317-329.

Clemente, R. and de la Torre, J.C. (2007). Cell-to-cell spread of Borna disease virus proceeds in the absence of the virus primary receptor and furin-mediated processing of the virus surface glycoprotein. *J Virol* **81,** 5968-5977.

Clemente, R. and de la Torre, J.C. (2009). Cell entry of Borna disease virus follows a clathrin-mediated endocytosis pathway that requires Rab5 and microtubules. *J Virol* **83,** 10406-10416.

Daito, T., Fujino, K., Honda, T., Matsumoto, Y., Watanabe, Y. and Tomonaga, K. (2011a). A novel borna disease virus vector system that stably expresses foreign proteins from an intercistronic noncoding region. *J Virol* **85,** 12170-12178.

Daito, T., Fujino, K., Watanabe, Y., Ikuta, K. and Tomonaga, K. (2011b). Analysis of intracellular distribution of Borna disease virus glycoprotein fused with fluorescent markers in living cells. *J Vet Med Sci* **73,** 1243-1247.

de la Torre, J.C. (1994). Molecular biology of borna disease virus: prototype of a new group of animal viruses. *J Virol* **68,** 7669-7675.

de la Torre, J.C. (2002). Molecular biology of Borna disease virus and persistence. *Front Biosci* **7,** d569-579.

Debaisieux, S., Encheva, V., Chakravarty, P., Snijders, A.P. and Schiavo, G. (2016). Analysis of Signaling Endosome Composition and Dynamics Using SILAC in Embryonic Stem Cell-Derived Neurons. *Mol Cell Proteomics* **15,** 542-557.

Deinhardt, K., Salinas, S., Verastegui, C., Watson, R., Worth, D., Hanrahan, S*., et al.* (2006). Rab5 and Rab7 control endocytic sorting along the axonal retrograde transport pathway. *Neuron* **52,** 293-305.

Diefenbach, R.J., Miranda-Saksena, M., Douglas, M.W. and Cunningham, A.L. (2008). Transport and egress of herpes simplex virus in neurons. *Rev Med Virol* **18,** 35-51.

Gonzalez-Dunia, D., Cubitt, B. and de la Torre, J.C. (1998). Mechanism of Borna disease virus entry into cells. *J Virol* **72,** 783-788.

Gonzalez-Dunia, D., Volmer, R., Mayer, D. and Schwemmle, M. (2005). Borna disease virus interference with neuronal plasticity. *Virus Res* **111,** 224-234.

Lalli, G., Bohnert, S., Deinhardt, K., Verastegui, C. and Schiavo, G. (2003). The journey of tetanus and botulinum neurotoxins in neurons. *Trends Microbiol* **11,** 431-437.

Lalli, G., Herreros, J., Osborne, S.L., Montecucco, C., Rossetto, O. and Schiavo, G. (1999). Functional characterisation of tetanus and botulinum neurotoxins binding domains. *J Cell Sci* **112 (Pt 16),** 2715-2724.

Lalli, G. and Schiavo, G. (2002). Analysis of retrograde transport in motor neurons reveals common endocytic carriers for tetanus toxin and neurotrophin receptor p75NTR. *J Cell Biol* **156,** 233-239.

Lennartz, F., Bayer, K., Czerwonka, N., Lu, Y., Kehr, K., Hirz, M*., et al.* (2016). Surface glycoprotein of Borna disease virus mediates virus spread from cell to cell. *Cell Microbiol* **18,** 340-354.

Lipkin, W.I., Briese, T. and Hornig, M. (2011). Borna disease virus - fact and fantasy. *Virus Res* **162,** 162-172.

Marra, P., Maffucci, T., Daniele, T., Tullio, G.D., Ikehara, Y., Chan, E.K*., et al.* (2001). The GM130 and GRASP65 Golgi proteins cycle through and define a subdomain of the intermediate compartment. *Nat Cell Biol* **3,** 1101-1113.

Mitchell, D.J., Blasier, K.R., Jeffery, E.D., Ross, M.W., Pullikuth, A.K., Suo, D*., et al.* (2012). Trk activation of the ERK1/2 kinase pathway stimulates intermediate chain phosphorylation and recruits cytoplasmic dynein to signaling endosomes for retrograde axonal transport. *J Neurosci* **32,** 15495-15510.

Prat, C.M., Schmid, S., Farrugia, F., Cenac, N., Le Masson, G., Schwemmle, M. and Gonzalez-Dunia, D. (2009). Mutation of the protein kinase C site in borna disease virus phosphoprotein abrogates viral interference with neuronal signaling and restores normal synaptic activity. *PLoS Pathog* **5,** e1000425.

Salinas, S., Bilsland, L.G., Henaff, D., Weston, A.E., Keriel, A., Schiavo, G. and Kremer, E.J. (2009). CAR-associated vesicular transport of an adenovirus in motor neuron axons. *PLoS Pathog* **5,** e1000442.

Salinas, S., Schiavo, G. and Kremer, E.J. (2010). A hitchhiker's guide to the nervous system: the complex journey of viruses and toxins. *Nat Rev Microbiol* **8,** 645-655.

Salomon, I., Janssen, H. and Neefjes, J. (2010). Mechanical forces used for cell fractionation can create hybrid membrane vesicles. *Int J Biol Sci* **6,** 649-654.

Schweizer, A., Fransen, J.A., Bachi, T., Ginsel, L. and Hauri, H.P. (1988). Identification, by a monoclonal antibody, of a 53-kD protein associated with a tubulo-vesicular compartment at the cis-side of the Golgi apparatus. *J Cell Biol* **107,** 1643-1653.

Taylor, M.P. and Enquist, L.W. (2015). Axonal spread of neuroinvasive viral infections. *Trends Microbiol* **23,** 283-288.

Wada, I., Rindress, D., Cameron, P.H., Ou, W.J., Doherty, J.J., 2nd, Louvard, D*., et al.* (1991). SSR alpha and associated calnexin are major calcium binding proteins of the endoplasmic reticulum membrane. *J Biol Chem* **266,** 19599-19610.

Wu, Y.J., Schulz, H., Lin, C.C., Saar, K., Patone, G., Fischer, H*., et al.* (2013). Borna disease virus-induced neuronal degeneration dependent on host genetic background and prevented by soluble factors. *Proc Natl Acad Sci U S A* **110,** 1899-1904.

Zhou, B., Cai, Q., Xie, Y. and Sheng, Z.H. (2012). Snapin recruits dynein to BDNF-TrkB signaling endosomes for retrograde axonal transport and is essential for dendrite growth of cortical neurons. *Cell Rep* **2,** 42-51.

Figure legends

Figure 1. BDV N and P colocalize with the binding fragment of tetanus neurotoxin (H_CT), a marker for axonal endosomes. Analysis of the colocalization between BDV N (A) or P (B) and H_CT by confocal microscopy. Upper panels: Hippocampal neurons were infected by BDV during 10 days before incubation with H_CT-555. BDV N (A) or P (B) proteins were detected by immunofluorescence (green signal) and the colocalization with H_CT-555 (red signal) was analyzed by confocal microscopy. Scale bar = 5 μm. Lower panels: Fluorescence intensity profiles of the green and red signals measured along the white arrow pictured on the upper corresponding image. (C) Quantification of the colocalization between BDV N or P with H_CT in axons. The histogram corresponds to the percentage of vesicles showing a colocalization between BDV proteins and H_CT-555. Data are expressed as means ± s. e. m. for: BDV N: 3 independent experiments, 23 fields and 210 BDV-containing vesicles; BDV P: 2 independent experiments, 21 fields and 171 BDV-containing vesicles.

Figure 2. Graphical overview of the methodologies employed to analyze the content of axonal endosomes. Method 1: Primary cortical neurons were infected or not with BDV, then submitted to either whole cell lysis, or a gentle lysis protocol designed to preserve the integrity of axonal endosomes. Extracts were then used in immunoprecipitation experiments using an anti-panTrk antibody, before western-blot analysis of the content of the immunoprecipitated fraction. Method 2: Primary cortical neurons were infected or not with BDV and incubated with H_CT-647. After gentle cell lysis, flow cytometry-based sorting of axonal endosomes was performed before analyzing the content of the positive-sorted fractions.

Figure 3. BDV proteins are found in immunoprecipitated axonal endosomes. Western blot analysis of the content of pan-Trk immunoprecipitated fractions. (A) Cortical neurons were infected (BDV) or not (NI) by BDV, then subjected to whole cell lysis before anti pan-Trk immunoprecipitation. Whole cell lysates (Input) or immunoprecipitated fractions (IP) were loaded onto SDS-PAGE before western blot using antibodies indicated on the left. Anti BDV G serum can detect the two isoforms of the protein, at 84 and 43 kDa. The star indicates a non-specific band, the arrowhead indicates the specific 84 kDa BDV G protein. (B) Cortical

neurons were infected (BDV) or not (NI) by BDV, then subjected to gentle cell lysis, preserving the integrity of axonal endosomes, before anti pan-Trk immunoprecipitation. Cell homogenates (Input) or immunoprecipitated fraction (IP) were loaded onto SDS-PAGE before western blot using the indicated antibodies. (C) Western blot analysis was performed on the same samples as (B) with the indicated antibodies, to control the purity of the axonal endosome preparations. Data shown are representative of one experiment out of five, that all provided similar results.

Figure 4. Flow cytometry analysis of fluorescent axonal endosomes. (A) Analysis of fluorescent vesicles obtained from non-infected neurons that were incubated with H_CT-647. Left panel: Crude fraction obtained after gentle lysis of neurons (acquired with instrument settings identical as those used for size standard beads) were size-gated into three populations designated P1 to P3. Right panels: Individual analyses of P1 to P3 populations, based on fluorescence intensity and counts. Numbers indicate the frequency of Alexa 647-positive events that were gated (right side of the graph) before sorting to obtain F1 and F2 fractions (no sorting was done on P3 population). Data shown are from one representative experiment out of four. (B) The same analysis was done on vesicles isolated from non-infected neurons that were not incubated with H_CT-647. In this case, no sorting was performed.

Figure 5. BDV proteins and genome are found in sorted axonal endosomes. Cortical neurons were infected (BDV) or not (NI) by BDV and subjected to gentle cell lysis before flow cytometry sorting and analysis. (A) Cell lysate before sorting (Input) or F1 sorted fraction (F1) were loaded onto SDS-PAGE before western blot using the indicated antibodies. The star indicates a non-specific band detected with the anti BDV M antibody. (B) Western blot analysis was performed on the same samples as in (A) with the indicated antibodies, to control the purity of axonal endosomes after sorting. Data shown are representative of one experiment out of two to four experiments. (C) Analysis of the presence of viral genome into sorted axonal endosomes by RT-PCR. Total RNAs were extracted from Input or F1 sorted fractions, reverse transcribed and analyzed by PCR using primers specific for viral genome. Amplified cDNAs were then loaded onto 1 % agarose gel. Mock: reverse-transcriptase was not added in the RT-PCR. MW: molecular weight ladder.

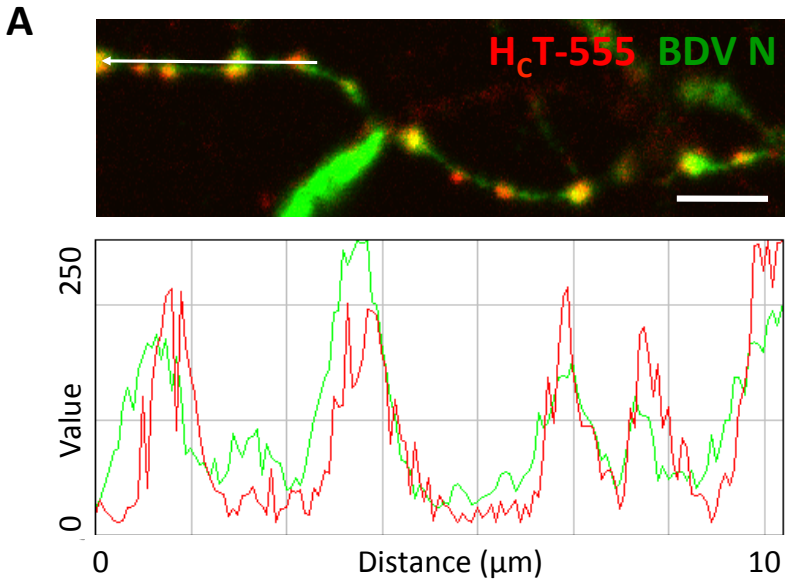
A
HcT-555 BDV N
250
Value
0
0
Distance (µm)
10

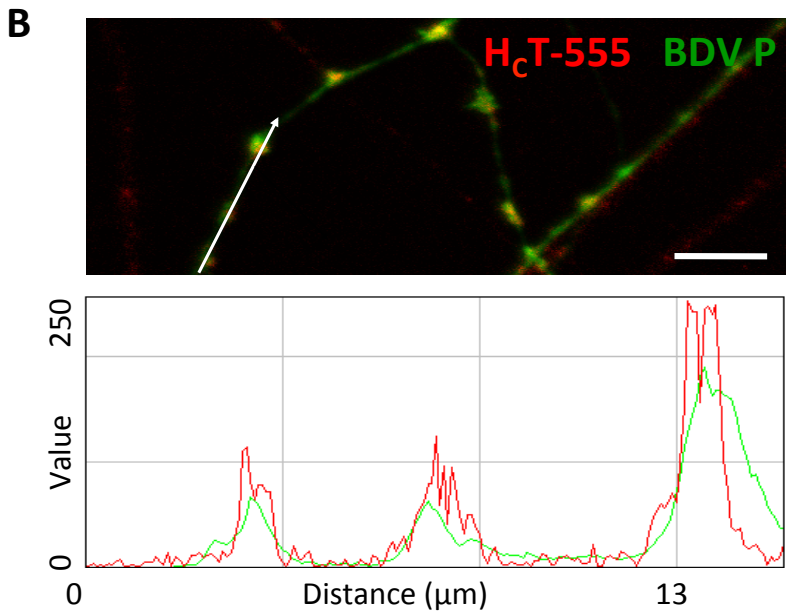
B
HcT-555 BDV P
250
Value
0
0
Distance (µm)
13

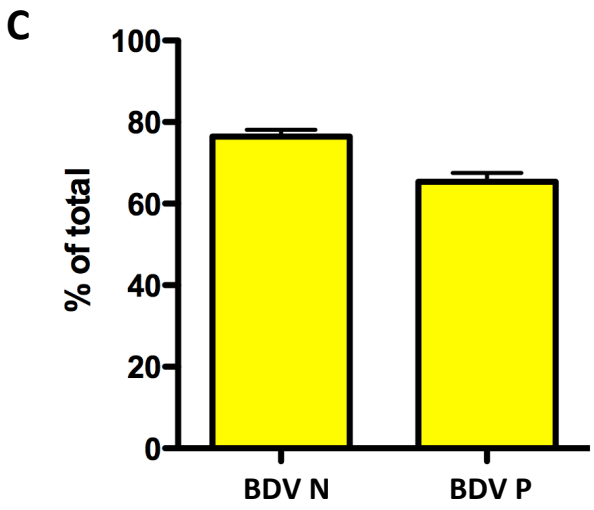
C
100
80
60
40
20
0
% of total
BDV N
BDV P

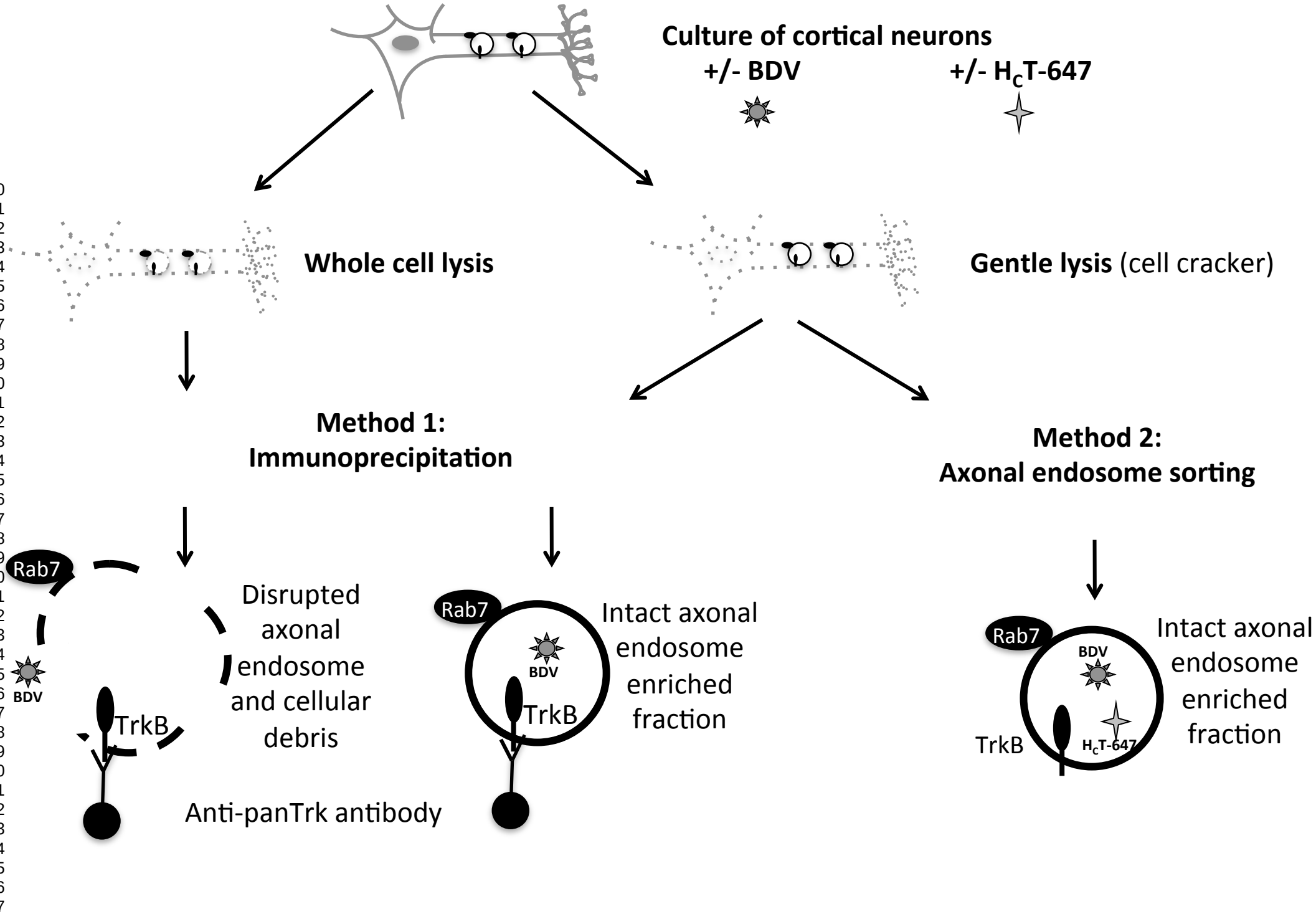
Culture of cortical neurons
+/- BDV
+/- HcT-647
Whole cell lysis
Gentle lysis (cell cracker)
Method 1:
Immunoprecipitation
Method 2:
Axonal endosome sorting
Rab7
BDV
TrkB
Disrupted axonal endosome and cellular debris
Anti-panTrk antibody
Intact axonal endosome enriched fraction
HcT-647

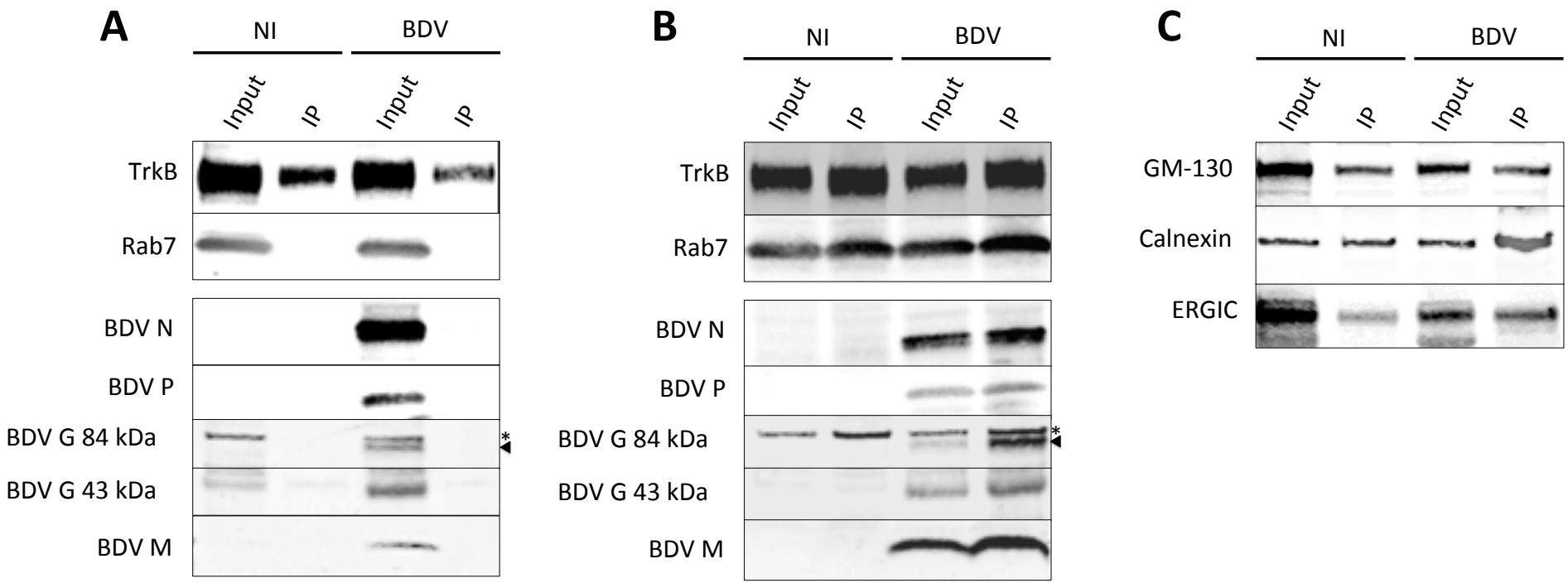
A
NI
BDV
Input
IP
Input
IP
TrkB
Rab7
BDV N
BDV P
BDV G 84 kDa
BDV G 43 kDa
BDV M
*
B
NI
BDV
Input
IP
Input
IP
TrkB
Rab7
BDV N
BDV P
BDV G 84 kDa
BDV G 43 kDa
BDV M
*
C
NI
BDV
Input
IP
Input
IP
GM-130
Calnexin
ERGIC

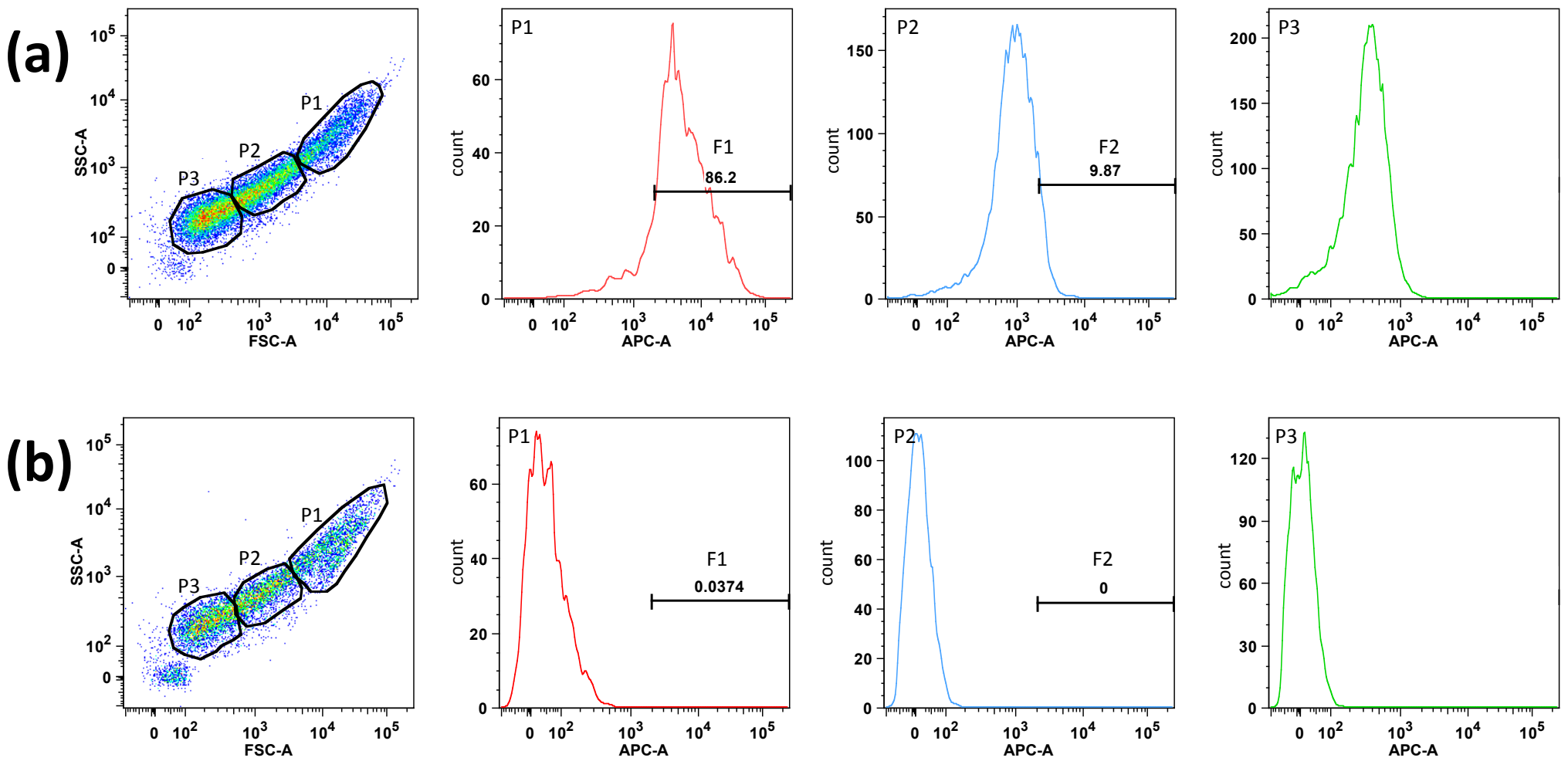
(a)
SSC-A
FSC-A
P1
P2
P3
count
APC-A
F1
86.2
F2
9.87
(b)
0.0374
0

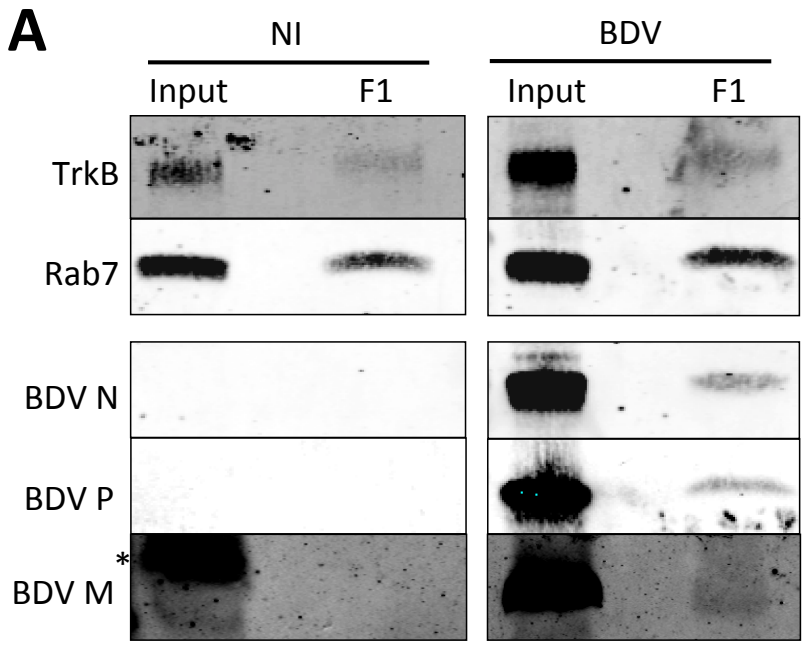
A
NI
BDV
Input
F1
Input
F1
TrkB
Rab7
BDV N
BDV P
*
BDV M

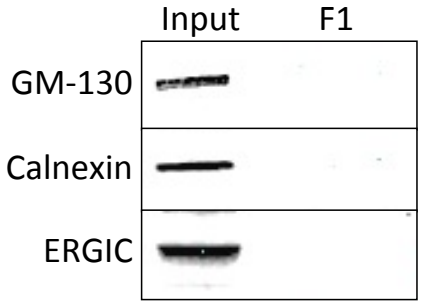
B
Input
F1
GM-130
Calnexin
ERGIC

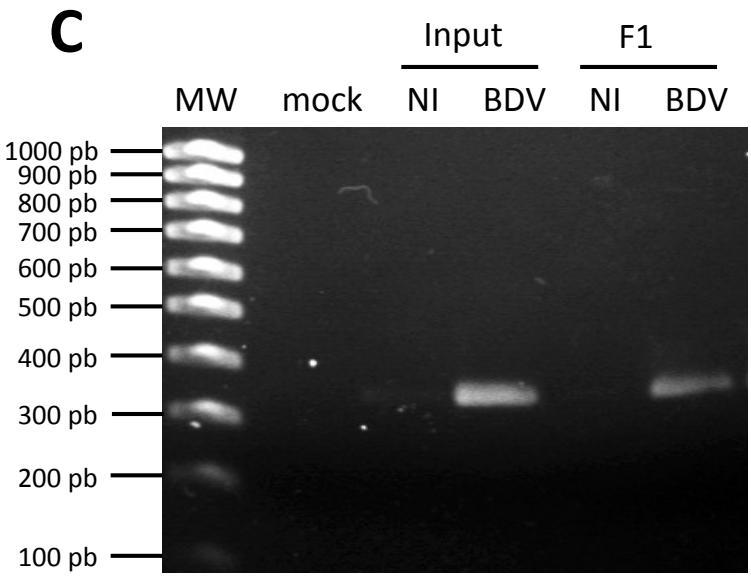
C
Input
F1
MW
mock
NI
BDV
NI
BDV
1000 pb
900 pb
800 pb
700 pb
600 pb
500 pb
400 pb
300 pb
200 pb
100 pb